Bioinformatics Analysis Reveals CCR7 As A Potential Biomarker for Predicting CKD Progression

Junju Lai
Division of Nephrology, The First Affiliated Hospital of Guangzhou Medical University, Guangzhou
Huizhi Shan
Division of Nephrology, The First Affiliated Hospital of Guangzhou Medical University, Guangzhou
Sini Cui
Division of Nephrology, The First Affiliated Hospital of Guangzhou Medical University, Guangzhou
Lingfeng Xiao
Division of Nephrology, The First Affiliated Hospital of Guangzhou Medical University, Guangzhou
Xiaowen Huang
Division of Nephrology, The First Affiliated Hospital of Guangzhou Medical University, Guangzhou
Yun Xiao (msxiaoyun@sina.com)
Division of Nephrology, The First Affiliated Hospital of Guangzhou Medical University, Guangzhou

Research Article

Keywords: Chronic kidney disease, Biomarker, CCR7

Posted Date: September 7th, 2021

DOI: https://doi.org/10.21203/rs.3.rs-730388/v1

Abstract

Background

Chronic kidney disease (CKD) inevitably progresses to end-stage renal disease if intervention does not occur in time. However, there are limitations in predicting the progression of CKD by solely relying on changes in renal function. A biomarker with high sensitivity and specificity that can predict the progression of CKD early is required.

Methods

We used the online Gene Expression Omnibus (GEO) microarray dataset GSE45980 to identify differentially expressed genes (DEGs) in patients with progressive and stable CKD. We then performed functional enrichment and protein-protein interaction (PPI) network analysis on DEGs and identified key genes. Finally, the expression patterns of the key genes were verified using the GSE60860 data set, and the receiver operating characteristic curve analysis was performed to clarify their predictive ability of progressive CKD. Ultimately, we verified the expression profiles of these hub genes in an in vitro renal interstitial fibrosis model by RT-PCR and western blot analysis.

Results

Differential expression analysis identified 50 upregulated genes and 47 downregulated genes. The results of the functional enrichment analysis revealed that the upregulated DEGs were mainly enriched in immune response, inflammatory response, and NF-κB signaling pathways, whereas the downregulated DEGs were mainly related to angiogenesis and the extracellular environment. PPI network and key gene analysis identified *CCR7* as the most important gene. *CCR7* mainly plays a role in immune response, and its only receptors, *CCL19* and *CCL21*, have also been identified as DEGs. The ROC curve analysis of *CCR7*, *CCL19* and *CCL21* found that *CCR7* and *CCL19* present good disease prediction ability.

Conclusion

CCR7 may be a stable biomarker for predicting the progression of CKD, and the *CCR7-CCL19/CCL21* axis may be a therapeutic target for end-stage renal disease. However, further experiments are needed to explore the relationship between these genes and CKD.

1. Introduction

Chronic kidney disease (CKD) affects 8–16% of the world's population [1]. Multiple regional epidemiological surveys indicate that the prevalence of CKD in China is around 10.8% [2]. Despite the high incidence of this disease, the general public does not fully understand the role the kidneys play in the human body and the consequences of kidney dysfunction. Recent statistical surveys indicate that less than 5% of the worldwide population know the function of the kidneys. In China, only 12.5% of the population is aware of the existence and implications of CKD [2, 3]. The rate of CKD progression is highly variable between individuals. In some patients, the renal function stabilizes and does not further deteriorate during several years (phase termed "stable CKD"), and in some cases it even improves over time ("reverse CKD"). Nonetheless, the majority CKD patients experience a decline in renal function over time ("progressive CKD").

Although some controversy exists around the need for early screening of CKD, it is undeniable that early intervention in CKD patients results in improved quality of life and reduces the consumption of medical resources [4]. Early studies suggested that glomerular filtration rate (GFR) decline follows a linear model, and that it could be used to predict when patients might reach end-stage renal disease (ESRD) and need renal replacement therapy [5, 6]. However, recent studies suggest that the progression of CKD is not linear, hindering prognosis prediction [7].

At present, it is still very difficult to predict or identify patients who will suffer from progressive CKD. This is caused by the lack of consensus on the definition of CKD progression, and more importantly, the lack of sensitive and specific biomarkers for early prediction of CKD progression. The most commonly used surrogate markers for CKD progression are proteinuria, serum creatinine levels and GFR, but these markers must be cautiously used as they present some limitations [8, 9]. Although recently some biomarkers have been considered as intermediate endpoints, such as renal injury molecules (KIM-1) [10], neutrophil gelatinase-associated protein (NGAL) [11] and soluble urokinase receptor (suPAR) [12], evidence about the utility of these markers in clinical practice is still lacking.

In this study, we used statistical analysis tools and data mining techniques to reveal gene patterns responsible for the progress of CKD. We mined biomarkers that can predict the progress of CKD. Here, we used the kidney tissue microarray dataset GSE45980 created by Rudnicki et al. to perform genome-wide gene expression analysis to study differentially expressed genes (DEGs) in patients with progressive CKD and stable CKD. Our research will help understand the genetic pattern of CKD progression and provide new insights for the clinical diagnosis and treatment of progressive CKD.

2. Materials And Methods

2.1 Microarray Data

The dataset GSE45980 with microarray expression data generated by Rudnicki et al. was downloaded from the Gene Expression Omnibus (GEO, https://www.ncbi.nlm.nih.gov/geo/). The dataset is based on the GPL13497 Agilent-026652 Whole Human Genome Microarray 4x44K v2 (Probe Name

version) array platform. The data set contained information about 43 kidney tissue samples from patients with different types of CKD. Twelve of these patients reached ESRD or doubled serum creatinine during follow-up were defined as progressive CKD patients, and the other 31 samples that did not meet the above criteria were defined as stable CKD patients. The annotation file for GPL13497 is also downloaded from GEO.

2.2 Differential Expression Analysis

DEG in progressive and stable CKD samples was analyzed by the limma package in Bioconductor [13]. The P-value of DEGs was calculated by using the unpaired Student's t-test using the limma package. We retained genes with the following criteria: (1) $|\log_2 FoldChange| > 0.5$, and (2) Adjusted P-values < 0.05. The heatmap package was used to draw the heatmap of the DEGs in R.

2.3 Functional Enrichment Analysis of DEGs

We used the online tool David 6.8 (https://david.ncifcrf.gov/tools.jsp) to analyze the functional categories in which the DEGs were enriched [14]. The functional categories Gene Ontology (GO) terms and Kyoto Encyclopedia of Genes and Genomes (KEGG) pathways were used for the enrichment analyses. GO is an commonly used tool for gene annotation that classifies the genes using a defined, structured and controlled vocabulary in three distinct categories, namely molecular function (MF), biological process (BP) and cellular components (CC) [15]. The KEGG is a database for assigning DEG groups to specific pathways [16]. We selected only genes with P-value < 0.05.

2.4 Protein-Protein Interaction (PPI) Network Analysis

PPI network analysis was performed using STRING (https://string-db.org/), an online database of known and predicted PPI [17]. We mapped DEGs to the PPI network using an interaction score > 0.4 as the threshold. The software of Cytoscape v3.6.0 was used to visualize and construct the PPI network [18]. Then, using the plug-in cytohubba we selected the hub genes by calculating and analyzing the network structure and the weighted connection between nodes using 12 algorithms [19].

2.5 Validation of the Hub Gene

We used the dataset GSE60860 uploaded to GEO by Rudnicki et al., which contains renal tissue samples from 8 patients with progressive CKD and 21 patients with stable CKD. We annotated the samples using the array platform GPL13497 Agilent-026652 Whole Human Genome Microarray 4x44K v2 (Probe Name version). We then used the limma package to identify the genes differentially expressed. Statistical analyses were performed using SPSS v19.0 software (SPSS Inc., Chicago, IL, USA). Student's t-test was used for statistical comparison, and Pearson correlation analysis was used for correlation analysis using age and gender as covariables. The receiver operating characteristic (ROC) curve was used to reflect the area under the curve (AUC) of hub genes to screen markers and evaluate their critical values. The significance levels were set at P < 0.05.

2.6 Cell culture

NRK-52E cells were obtained from Jinan University (Guangdong, China) and were cultured in Dulbecco's Modified Eagle Medium (DMEM. GIBCO BRL, Life Technologies Inc., Gaithersburg, MD, USA) with 10% Fetal Bovine Serum (FBS, GIBCO BRL) at 37 ° C and 5% CO2. NRK-52E cells were seeded in 6-well plates. When the cells confluence reached 60% – 70%, they were transferred to serum-free medium and starved for 24 h. Recombinant human TGF-β1 at a final concentration of 10 ng / ml was subsequently added to the culture medium, and cultured for 0, 6, 12, and 24 h.

2.7 Quantitative real-time PCR

Total RNA was extracted from NRK-52E cells using TRIzol reagent (Invitrogen) according to the manufacturer's instructions. cDNA was synthesized from equal amounts of RNA using reverse transcriptase purchased from Takara Bio Inc. (Shiga, Japan). The specific primers for the target genes were designed by GENEray (Shanghai, China) and synthesized according to the GeneBank sequences cDNA was amplified by PCR using specific pairs of primers. The reaction system was formulated in compliance with the specifications of SYBR Premix EX Taqkits (Takara bio Inc.). The reaction conditions were: pre denaturation at 95º C for 30 s, denaturation at 95º C for 5 s, annealing at 58º C to 60º C (depending on the specific pair of primers used), extension for 10 s for 40 cycles, and then annealing at 95º C for 15 s. mRNA expression was calculated according to the standard curve, using expression levels of *GAPDH* as the internal control. Primer sequences were as follows: *CCR7* (forward: 5'-TGTACGAGTCGGTGTGCTTC-3'; reverse: 5'- GGTAGGTATCCGTCATGGTCTTG-3'), *FN* (forward: 5'-GTGTCCTCCTTCCATCTTC-3'; reverse: 5'-CAGACTGTCGGTACTCACG-3'), *GAPDH* (forward: 5'- AGGTCGGTGTGAACGGATTTG-3'; reverse: 5'-TGTAGACCATGTAGTTGAGGTCA-3').

2.8 Protein extraction and western blot analysis

NRK-52E cells were lysed with RIPA lysis buffer on ice and centrifuged. Protein concentrations were determined by enzyme-linked immunoassay (Bio-Rad) and equilibrated with RIPA buffer. Proteins were separated on 10% SDS-PAGE gels and transferred to nitrocellulose membranes (Millipore, Billerica, MA, USA). Membranes were sealed in 5% non-fat milk for 2 h at room temperature. After three times TBS-T washes, membranes were incubated with the corresponding primary antibodies (rabbit polyclonal anti-CCR7 antibodies (Proteintech, 1:1000), rabbit polyclonal anti-GAPDH, FN antibodies (Cell Signaling Technologies, 1:1000)) overnight at 4º C. Then, membranes were rinsed three times with TBS-T, and incubated with horseradish peroxide intensified secondary antibodies for 2 h. Protein expression levels were detected and imaged generated using the Odyssey CLX Imaging System (LI-COR, Lincoln, NE, USA).

2.9 Statistical analysis

Data are presented as mean ± standard error of mean (SEM) indicates. Statistical tests were performed using SPSS 16.0 statistical software (SPSS Inc., Chicago, IL, USA). Unpaired Student's t-test was used to compare means between two groups. One-way ANOVA and LSD test were used for comparison of multiple groups. P-values less than 0.05 were considered statistically significant.

3. Results

3.1 Genes differentially expressed between progressive and stable CKD patient samples.

We downloaded the microarray expression dataset GSE45980 from the GEO database and analyzed the DEGs in progressive and stable CKD samples. A total of 50 upregulated genes and 47 downregulated genes were identified between patients with progressive and stable CKD (Fig. 1). The top ten significantly upregulated and downregulated genes are listed in Table 1 ranked by $\log_2$FoldChange value.

3.2 Functional and Pathway Enrichment of DEGs

We then analyzed the pathway and functions in which the identified DEGs were enriched. A total of 22 significantly enriched GO terms and 4 KEGG pathways were identified. The upregulated DEGs were mainly enriched in the GO terms related to the immune response, inflammatory response, and NF-κB signaling pathway, whereas the downregulated DEGs were mainly related to angiogenesis and the extracellular environment (Table 2). In addition, the upregulated DEGs were in the KEGG pathways chemokine signaling pathway, cytokine-cytokine receptor interaction, and NF-κB signaling pathway. Down-regulated DEGs were significantly enriched in vascular smooth muscle contraction (Table 3).

3.3 PPI Network Analysis of DEGs

A PPI network with 55 nodes and 116 edges, and interaction score of the network > 0.4 was generated using the tools STRING and Cytoscape (Fig. 2A). In the generated network, each node represents one gene, and edges represent links between genes. Up-regulated genes are depicted in red, whereas downregulated genes are depicted in green. Analysis of the key modules of the network revealed that there were two main modules, which included five upregulated genes (*CCR7, CCL19, CCL21, CXCL1* and *S1PR4*) and nine downregulated genes (*KNG1,CALD1、MYH11、TPM2、MYLK、TAGLN、MYL9、ACTA2*, and *CSRP1)* (Fig. 2B, C). The hub genes were then determined using 12 distinct calculation methods (Table 4). The gene with the highest repetition rate was *CCR7* (in the 12 calculation methods, 10 times appeared in the top 10 genes).

3.4 Identification of Genes of Interest and Validation of the several DEGs using other datasets

The only ligands of the protein encoded by *CCR7*, which was identified as the most important gene, are CCL19 and CCL21 [20]. Both *CCL19* and *CCL21* were identified as upregulated DEGs. Enrichment analysis showed that these three genes were enriched in immune response, inflammatory response, and NF-κB signaling pathway, all of which are important pathways for the progression of CKD to end-stage renal disease.

To verify the expression levels of the three genes identified as potentially important DEGs in the progression to end-stage renal disease, we analyzed their expression levels in the dataset GSE60860. In this dataset, a total of 154 DEGs were identified. We closely monitored the expression levels of *CCR7* ($P < 0.05$), *CCL21* ($P < 0.05$), and *CCL19* ($P < 0.05$), and compared their expression in the dataset (Fig. 3A). Spearman correlation analysis showed that *CCR7, CCL21* and *CCL19* expression levels were not significantly correlated with age and gender (Table 5).

In addition, we evaluated the potential utility of using *CCR7*, *CCL21*, and *CCL19* expression levels as biomarkers using ROC curves generated with the two datasets (Fig. 3B). The AUC of *CCR7* was 0.767 ($P < 0.01$, 95% CI = 0.645–0.889), and the sensitivity and specificity of predicting CKD progression were 0.65 and 0.788, respectively. The AUC of *CCL19* was 0.755 ($P < 0.001$, 95% CI = 0.635–0.874), and the sensitivity and specificity were 0.900 and 0.635. Finally, the AUC of *CCL21* was 0.629 ($P > 0.05$). The results showed that both *CCR7* and *CCL19* had a good predictive ability. The lower AUC of *CCL21* might be caused by the number of samples.

3.5 Validation of CCR7 expression in an in vitro renal interstitial fibrosis model.

To further validate the relationship between *CCR7* expression levels and CKD severity, we examined the expression of *CCR7* using an *in vitro* model of renal interstitial fibrosis. We used TGF-β1-stimulated NRK-52E cells to model renal interstitial fibrosis. To model the progression of CKD to end-stage renal disease, we used longer TGF-β1 stimulation times. Analysis of the mRNA and protein expression levels using RT-qPCR and Western Blot revealed that the protein and mRNA expression levels of FN and CCR7 gradually increased with the duration of TGF-β1 stimulation. The observed increased was especially notable at 24 h and 48 h (Fig. 4). The expression levels of FN and CCR7 were positively correlated.

4. Discussion

In this study, 97 DEGs, of which 50 were upregulated and 47 were downregulated, were identified in progressive CKD samples compared with stable CKD samples in the array dataset GSE45980. Enrichment analysis showed that upregulated DEGs were significantly enriched in pathways related to the immune response, inflammatory response, and NF-κB signaling pathway, which was also recognized as the key process for the progression of CKD to end-stage renal disease. The gene *CCR7*, which was upregulated in progressive CKD samples, was enriched in the above GO-terms and KEGG pathways, and presented the highest interaction degree in the PPI network. Using an *in vitro* model of renal interstitial fibrosis model, we identified that the expression level of CCR7 was concomitantly increased with the aggravation of oxidative stress.

Chemokines play a key role in numerous immune processes, including immune cell development, immune response initiation, and the pathophysiological recruitment of immune cells in infections and diseases. Functionally, chemokines can be divided into two categories: inflammatory chemokines, which are mainly expressed during activation of the immune response, and steady-state chemokines, which are constitutively expressed in discrete locations without obvious activation stimuli [21]. Nonetheless, most chemokines have both functions. CCR7 is an essential chemokine necessary to maintain homeostasis. Under homeostatic conditions, low levels of CCR7 in the lymph nodes contributes to peripheral tolerance. However, when encountering inflammatory mediators, pathogens or tissue damage, dendritic cells (DCs) express high amounts of CCR7, which in turn induces an immune response [20, 22].

CCR7 has only two constitutive ligands, CCL19 (also known as Eb11 ligand chemokine or ELC) and CCL21 (also known as secondary lymphochemokine or SLC). CCL21 has a distinctive 32 amino acids-long C-terminal tail. Twelve of the C-terminal amino acids are basic amino acid residues that can bind to glycosaminoglycans and other molecules [23]. Whereas CCL21 mediates the migration effects in CCR7, CCL19 plays a complementary role and mediates non-migration signals, such as promoting cell survival [24]. Both these ligands, CCL21 and CCL19, were also identified as upregulated DEGs.

The CCR7-CCL19/CCL21 axis can promote the retention of $CD4^+$ T lymphocytes at the reconstruction site of collateral arteries, thereby promoting arteriogenesis [25]. Liu et al. found that Baicalin inhibited the levels of CCR7 and NF-κB simultaneously when studying the anti-inflammatory mechanism of Baicalin in asthma [26]. Qian et al. found that Newcastle disease virus-like particles (NDV VLPs) activate DCs through TLR4/NF-κB pathway, and promote DC migration through the CCR7-CCL19/CCL21 axis [27]. These results show that CCR7-CCL19/CCL21 axis may be related to the NF-κB pathway, which plays an important role in the cellular inflammatory response and immune response [28]. In addition, McNamee et al. found that CCL19, CCL21 and CCR7 were involved in the induction and maintenance of chronic inflammation in a Crohn's-like ileitis mice model [29]. These results are consistent with the results of the GO term and KEGG pathways enrichment analysis.

Several studies have found that CCL21 and CCR7 are expressed in interstitial fibroblasts and tubular epithelial cells in transplanted kidneys [30], and the CCL21-CCR7 axis can promote renal fibrosis [31]. Early studies have shown that lymph angiogenesis is closely related to the progression of tubulointerstitial fibrosis [32]. Pei et al. identified that that lymphatic vessels were significantly increased in CKD biopsy samples relative to normal samples [33]. In addition, CCL21 was highly expressed in lymphatic vessels, with $CCR7^+$ lymphocytes and DCs clustered near lymphatic vessels. The same results were observed in unilateral ureteral obstruction animal models, in which blocking CCR7 inhibits lymph angiogenesis and reduces injury-induced inflammation and fibrosis. These results suggest that the recruitment of lymphocytes and DC in the kidney depends on the CCL21-CCR7 axis. Altogether, these results indicate that continuous damage to the kidney leads to lymphatic vessels angiogenesis and the recruitment $CCR7^+$ cells into the kidney, which in turn and accelerates intrarenal inflammation. This suggests that there is a relationship between the expression level of CCR7 and the severity of CKD. Studies have found that CCL19 can inhibit cell viability and promote cellular inflammation and fibrosis in DN cells [34]. Mesenchymal stem cells can also inhibit renal inflammation by reducing the expression levels of CCL19 [35]. At present, there are few reports about CCL19, since the CCL19-CCR7 axis is commonly overlooked in comparison with the CCL21-CCR7 axis. However, recent reports show that the CCL19-CCR7 axis plays an important role in renal inflammation. Limited sample data and related experimental results show that, compared with CCR7, CCL19 and CCL21 are still unstable markers for predicting the progress of CKD.

In conclusion, CCR7 may play an important role in the progression of CKD through the immune system. The expression level of CCR7 may be related to the severity of CKD. We found that the expression level of CCR7 was independent of gender and age, indicating that it may be a prognostic marker for CKD progression in individuals of different age and gender. However, more experiments and larger multicenter prospective studies are required to validate the utility of this marker, as well as the threshold for predicting CKD progression and adverse events. As the only ligands of CCR7, the roles of CCL19 and CCL21 in the progression of CKD still need further study. Recent results indicate that the CCR7-CCL19/CCL21 axis may be a therapeutic target for chronic kidney disease and end-stage renal disease.

Declarations

Ethics approval and consent to participate

The datasets from the GEO database has been approved by the Institutional Review Board of the Medical University of Innsbruck.

Consent for publication

Not applicable.

Availability of data and materials

The datasets in the current study come from CEO database: GSE45980 and GSE60860.

Competing interests

The authors declare that they have no competing interests.

Funding

National Natural Science Foundation of China. (Grant No. 81600538)

Authors' contributions

J.L. designed the study, Y.X. supervised the study, J.L. and H.S. drafted the manuscript, S.C., L.X. and X.H. collected data. The author(s) read and approved the final manuscript.

Acknowledgements

We would like to thank Editage (www.editage.cn) for English language editing.

References

1. Chen, T.K., D.H. Knicely and M.E. Grams, Chronic Kidney Disease Diagnosis and Management: A Review. JAMA, 2019. 322(13): p. 1294–1304.
2. Zhang, L., et al., Prevalence of chronic kidney disease in China: a cross-sectional survey. Lancet, 2012. 379(9818): p. 815 – 22.
3. Tuot, D.S., et al., Chronic Kidney Disease Awareness Among Individuals with Clinical Markers of Kidney Dysfunction. Clinical Journal of the American Society of Nephrology, 2011. 6(8): p. 1838–1844.
4. Levin, A. and P.E. Stevens, Early detection of CKD: the benefits, limitations and effects on prognosis. Nat Rev Nephrol, 2011. 7(8): p. 446 – 57.
5. Mitch, W.E., et al., A simple method of estimating progression of chronic renal failure. Lancet, 1976. 2(7999): p. 1326-8.
6. Modification Of Diet In Renal Disease Study Group, et al., Predictors of the progression of renal disease in the Modification of Diet in Renal Disease Study. Kidney International, 1997. 51(6): p. 1908–1919.
7. Li, L., et al., Longitudinal Progression Trajectory of GFR Among Patients With CKD. American Journal of Kidney Diseases, 2012. 59(4): p. 504–512.
8. Glassock, R.J., Debate: CON Position. Should Microalbuminuria Ever Be Considered as a Renal Endpoint in Any Clinical Trial. American Journal of Nephrology, 2010. 31(5): p. 462–465.
9. Coresh, J., et al., Decline in Estimated Glomerular Filtration Rate and Subsequent Risk of End-Stage Renal Disease and Mortality. JAMA, 2014. 311(24): p. 2518.
10. Sabbisetti, V.S., et al., Blood kidney injury molecule-1 is a biomarker of acute and chronic kidney injury and predicts progression to ESRD in type I diabetes. Journal of the American Society of Nephrology, 2014. 25(10): p. 2177–2186.
11. Bolignano, D., et al., Neutrophil Gelatinase-Associated Lipocalin (NGAL) and Progression of Chronic Kidney Disease. Clinical Journal of the American Society of Nephrology, 2009. 4(2): p. 337–344.
12. Hayek, S.S., et al., Soluble Urokinase Receptor and Chronic Kidney Disease. N Engl J Med, 2015. 373(20): p. 1916-25.
13. Ritchie, M.E., et al., limma powers differential expression analyses for RNA-sequencing and microarray studies. Nucleic Acids Research, 2015. 43(7): p. e47-e47.
14. Huang, D.W., B.T. Sherman and R.A. Lempicki, Systematic and integrative analysis of large gene lists using DAVID bioinformatics resources. Nat Protoc, 2009. 4(1): p. 44–57.
15. Ashburner, M., et al., Gene Ontology: tool for the unification of biology. Nature Genetics, 2000. 25(1): p. 25–29.
16. Kanehisa, M. and S. Goto, KEGG: kyoto encyclopedia of genes and genomes. Nucleic Acids Res, 2000. 28(1): p. 27–30.
17. Szklarczyk, D., et al., The STRING database in 2017: quality-controlled protein–protein association networks, made broadly accessible. Nucleic Acids Research, 2017. 45(D1): p. D362-D368.
18. Shannon, P., et al., Cytoscape: a software environment for integrated models of biomolecular interaction networks. Genome Res, 2003. 13(11): p. 2498 – 504.
19. Chin, C., et al., cytoHubba: identifying hub objects and sub-networks from complex interactome. BMC systems biology, 2014. 8 Suppl 4(Suppl 4): p. S11.
20. Förster, R., A.C. Davalos-Misslitz and A. Rot, CCR7 and its ligands: balancing immunity and tolerance. Nature Reviews Immunology, 2008. 8(5): p. 362–371.
21. Zlotnik, A. and O. Yoshie, The chemokine superfamily revisited. Immunity, 2012. 36(5): p. 705 – 16.
22. Ohl, L., et al., CCR7 governs skin dendritic cell migration under inflammatory and steady-state conditions. Immunity, 2004. 21(2): p. 279 – 88.
23. Yoshida, R., et al., Secondary lymphoid-tissue chemokine is a functional ligand for the CC chemokine receptor CCR7. J Biol Chem, 1998. 273(12): p. 7118-22.
24. Comerford, I., et al., A myriad of functions and complex regulation of the CCR7/CCL19/CCL21 chemokine axis in the adaptive immune system. Cytokine Growth Factor Rev, 2013. 24(3): p. 269 – 83.
25. Nossent, A.Y., et al., CCR7-CCL19/CCL21 Axis is Essential for Effective Arteriogenesis in a Murine Model of Hindlimb Ischemia. J Am Heart Assoc, 2017. 6(3).
26. Liu, J., et al., Baicalin attenuates inflammation in mice with OVA-induced asthma by inhibiting NF-kappaB and suppressing CCR7/CCL19/CCL21. Int J Mol Med, 2016. 38(5): p. 1541–1548.
27. Qian, J., et al., Newcastle disease virus-like particles induce DC maturation through TLR4/NF-kappaB pathway and facilitate DC migration by CCR7-CCL19/CCL21 axis. Vet Microbiol, 2017. 203: p. 158–166.
28. Sun, S.C., The non-canonical NF-kappaB pathway in immunity and inflammation. Nat Rev Immunol, 2017. 17(9): p. 545–558.
29. McNamee, E.N., et al., Ectopic lymphoid tissue alters the chemokine gradient, increases lymphocyte retention and exacerbates murine ileitis. Gut, 2013. 62(1): p. 53–62.
30. Zhou, H.L., et al., Distribution and expression of fibroblast-specific protein chemokine CCL21 and chemokine receptor CCR7 in renal allografts. Transplant Proc, 2013. 45(2): p. 538 – 45.
31. Sakai, N., et al., Secondary lymphoid tissue chemokine (SLC/CCL21)/CCR7 signaling regulates fibrocytes in renal fibrosis. Proc Natl Acad Sci U S A, 2006. 103(38): p. 14098-103.
32. Sakamoto, I., et al., Lymphatic vessels develop during tubulointerstitial fibrosis. Kidney Int, 2009. 75(8): p. 828 – 38.
33. Pei, G., et al., Lymphangiogenesis in kidney and lymph node mediates renal inflammation and fibrosis. Science advances, 2019. 5(6): p. eaaw5075.
34. Sun, J., et al., MiR-325-3p inhibits renal inflammation and fibrosis by targeting CCL19 in diabetic nephropathy. Clin Exp Pharmacol Physiol. 2020;47(11):1850–1860.

35. Kim, H.S., et al., Mesenchymal Stem Cells Ameliorate Renal Inflammation in Adriamycin-induced Nephropathy. Immune Netw, 2019. 19(5): p. e36.

Tables

Table 1
Top ten up- and downregulated gene

Upregulated genes			Downregulated genes		
Gene symbol	logFC	adj.P.Val	Gene symbol	logFC	adj.P.Val
TBC1D10C	1.270903	0.012108	ACTA2	-1.283903	0.019401
REG1A	1.266544	0.021584	MYH11	-1.198393	0.047796
CCL19	1.260658	0.047002	KNG1	-1.004037	0.033276
IL7R	1.199639	0.029889	DCN	-0.874742	0.043624
LTB	1.164515	0.021584	MGP	-0.872574	0.021584
JAK3	1.082178	0.012437	LPL	-0.8698	0.04524
CCL21	1.07003	0.04524	EMCN	-0.852292	0.04524
PIGR	1.034732	0.041715	TIMP3	-0.847645	0.013315
CCR7	1.034619	0.021584	TAGLN	-0.831096	0.021584
RASAL3	0.999338	0.010765	TMEM204	-0.830443	0.013315

Table 2
GO analysis of differentially expressed genes (P < 0.05,count ≥ 4).

GO-ID	Term	Count	PValue	Genes
Upregulated genes				
GO-BP terms				
GO:0006955	immune response	9	1.17E-05	CXCL1, CCR7, TNFRSF25, CCL21, S1PR4, IRF8, CCL19, IL7R, LTB
GO:0090023	positive regulation of neutrophil chemotaxis	4	2.50E-05	CXCL1, CCR7, CCL21, CCL19
GO:0006954	inflammatory response	7	4.34E-04	CXCL1, CCR7, TNFRSF25, CCL21, RELB, CCL19, ADAM8
GO:0051897	positive regulation of protein kinase B signaling	4	0.001379	CCR7, CCL21, CCL19, ADAM8
GO:0043123	positive regulation of I-kappaB kinase/NF-kappaB signaling	4	0.008592	CCR7, CCL21, CCL19, BIRC3
GO:0007165	signal transduction	8	0.030044	CXCL1, CLDN3, TNFRSF25, RASGRP2, RASAL3, IL7R, LTB, ARHGAP9
GO:0007166	cell surface receptor signaling pathway	4	0.034825	TNFRSF25, CD2, BIRC3, IL7R
GO-CC terms				
GO:0005578	proteinaceous extracellular matrix	4	0.033472	HAPLN3, CCL21, ADAMTS10, PAPLN
GO-MF terms				
GO:0005102	receptor binding	5	0.010352	CXCL1, TMC8, CD2, JAK3, LTB
GO:0008270	zinc ion binding	8	0.02123	MICALL2, ZMIZ2, ZSWIM7, ADAMTS10, PAPLN, BIRC3, ADAM8, SP140
Downregulated genes				
GO-BP terms				
GO:0006936	muscle contraction	6	9.54E-06	ACTA2, CALD1, MYH11, TPM2, MYLK, MYL9
GO:0001525	angiogenesis	5	0.002945	EMCN, EPAS1, TEK, MCAM, RAMP1
GO-CC terms				
GO:0031012	extracellular matrix	8	7.43E-06	LPL, NES, RARRES2, HTRA1, LGALS1, MGP, DCN, TIMP3
GO:0070062	extracellular exosome	18	2.17E-04	KNG1, TPPP3, LPL, RARRES2, ACTA2, LGALS1, C16ORF89, MGP, CSRP1, TIMP3, DUSP26, HTRA1, CLIC5, MYH11, VAMP5, PRSS23, MGAT5, MYLK
GO:0005615	extracellular space	10	0.005019	KNG1, DKK3, LPL, HTRA1, ACTA2, LGALS1, DCN, MCAM, TIMP3, RAMP1
GO:0005576	extracellular region	11	0.005093	KNG1, DKK3, LPL, EMCN, RARRES2, HTRA1, NELL1, TEK, ANTXR2, DCN, TIMP3
GO:0009986	cell surface	6	0.010474	LPL, LGALS1, TEK, VAMP5, RAMP1, AOC3
GO-MF terms				
GO:0003779	actin binding	4	0.031639	TAGLN, CALD1, TPM2, MYLK

Table 3
KEGG pathway enrichment analyses for differentially expressed genes (P < 0.05,Count ≥ 4).

ID	Description	Count	PValue	Genes
Upregulated genes				
hsa04062	Chemokine signaling pathway	7	1.39E-05	CXCL1, CCR7, CCL21, RASGRP2, CCL19, JAK3, PLCB2
hsa04060	Cytokine-cytokine receptor interaction	7	6.34E-05	CXCL1, CCR7, TNFRSF25, CCL21, CCL19, IL7R, LTB
hsa04064	NF-kappa B signaling pathway	5	1.21E-04	CCL21, RELB, CCL19, BIRC3, LTB
Downregulated genes				
hsa04270	Vascular smooth muscle contraction	5	3.80E-04	ACTA2, CALD1, RAMP1, MYLK, MYL9

Table 4
Hub genes ranked in cytoHubba

Rank methods in cytoHubba											
MCC	DMNC	MNC	Degree	EPC	BottleNeck	EcCentricity	Closeness	Radiality	Betweenness	Stress	ClusteringCoefficien
TAGLN	ACTA2	CCR7	CCR7	CCR7	PLCB2	PLCB2	CCR7	IKZF1	TEK	KNG1	JAK3
MYH11	MYLK	CCL19	S1PR4	CCL19	TEK	KNG1	IKZF1	KNG1	KNG1	TEK	LGALS1
ACTA2	TPM2	S1PR4	IKZF1	S1PR4	KNG1	RASGRP2	S1PR4	CCR7	IKZF1	IKZF1	ARHGAP9
MYLK	MYL9	IKZF1	CCL19	IKZF1	IKZF1	DCN	KNG1	S1PR4	PLCB2	PLCB2	CALD1
TPM2	CSRP1	TAGLN	TAGLN	KNG1	TAGLN	PRSS23	CCL19	CCL19	ACTA2	S1PR4	CSRP1
MYL9	CALD1	MYH11	ACTA2	CXCL1	CCR7	COX7A1	IRF8	PLCB2	S1PR4	ACTA2	NES
CSRP1	KNG1	ACTA2	KNG1	CCL21	RUNX3	TEK	CXCL1	IRF8	TAGLN	TIMP3	MYL9
CALD1	TAGLN	MYLK	MYH11	RELB	TIMP3	IKZF1	CCL21	CXCL1	TIMP3	CCR7	TPM2
CCR7	MYH11	TPM2	MYLK	CD2	ACTA2	CCR7	WDFY4	CCL21	DCN	TAGLN	CCL21
CCL19	CXCL1	MYL9	TPM2	IRF8	S1PR4	TIMP3	ACTA2	TIMP3	CCR7	DCN	CXCL1

MCC: Maximal cilque centrality; MNC:Maximum neighborhood component; Degree: Node connect degree; EPC: Edge percolated component.

Table 5
Correlation analysis of CCR7, CCL21, CCL19 with gender and age

		Age		Gender	
		r_s	p	r_s	p
Spearman's rho	CCR7	0.109	0.361	-0.155	0.195
	CCL21	-0.172	0.148	0.1	0.403
	CCL19	0.143	0.23	-0.003	0.977

r_s,Spearman's rank correlation coefficient

Figures

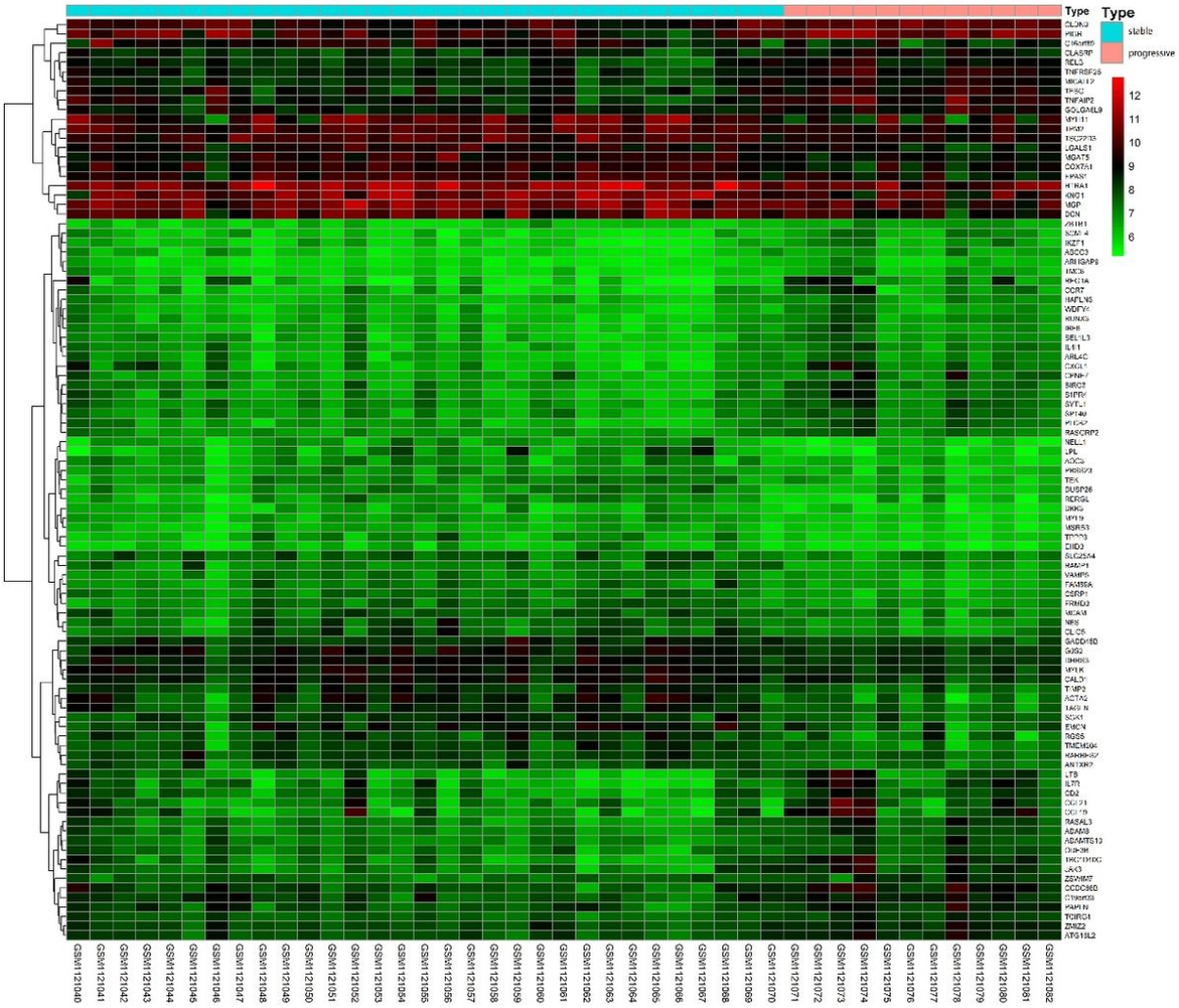

Figure 1

Heatmap of 97 differentially expressed genes were detected in 31 stable CKD patients and 12 progressive CKD patients. Red represents upregulated genes and the green represents downregulated genes.

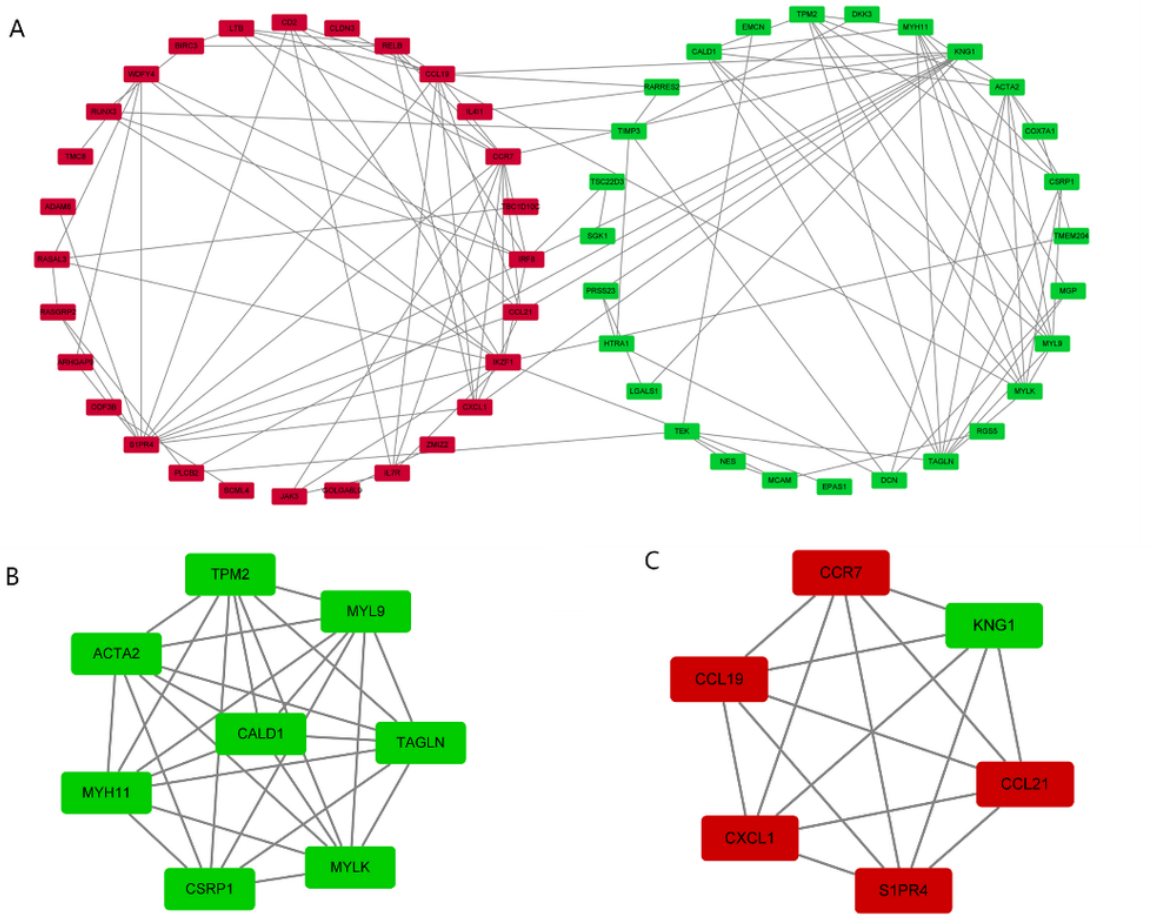

Figure 2

(A) According to the STRING online database, a visual network of 55 nodes and 116 edges was obtained with an interaction score > 0.4. Nodes represent genes, and edges represent connections between genes. Up-regulated genes are represented in red, whereas downregulated genes are represented in green. (B, C) Two key modules for identifying network gene clustering were identified with MCODE.

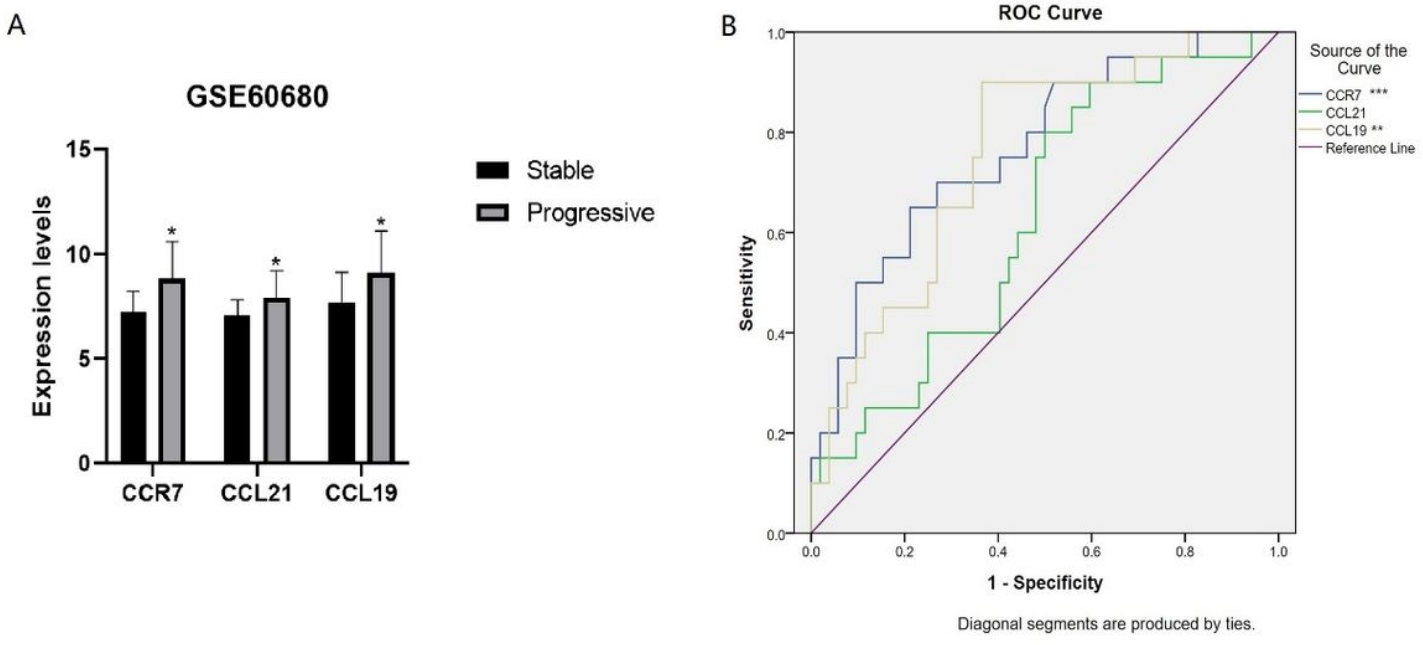

Figure 3

(A) Expression levels of CCR7, CCL21 and CCL19. (B) ROC curve analysis of CCR7, CCL21 and CCL19 in two data sets. Significance is represented as *, P<0.05; **, P < 0.01; ***, P < 0.00.

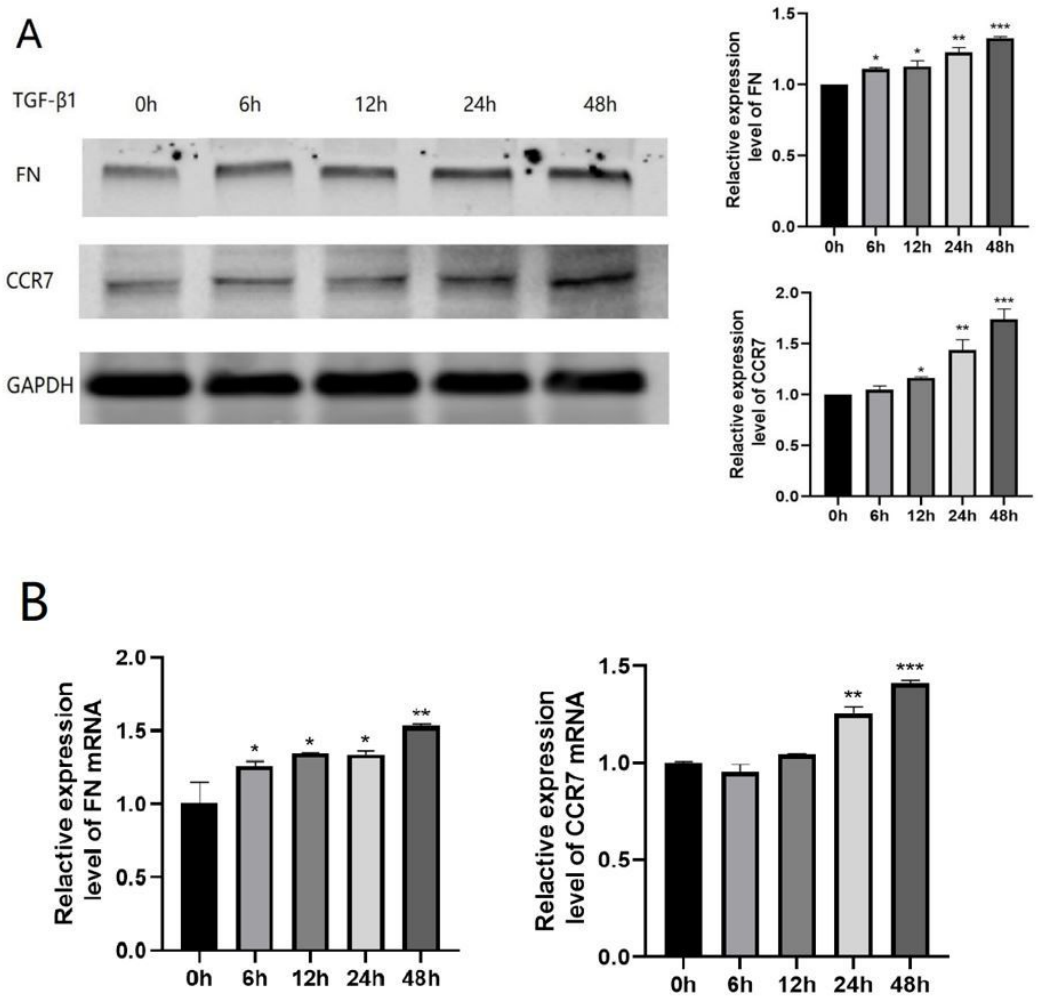

Figure 4

Expression levels of key genes in NRK-52E cells. Cells were treated with 10 ng/mL TGF-β1 for 0, 6, 12, 24, and 48 hours. (A) FN and CCR7 protein expression levels were analyzed by western blot. (B) FN and CCR7 mRNA levels were analyzed by real-time PCR. Results are presented as the mean ± standard error of three independent experiments. (*, P<0.05; **, P < 0.01; ***, P < 0.001 vs 0h)